New Concept for the Effect of Metal Particle Size
on the Catalyst Activity
in the Reactions Involving Oxygen

By

Tomoyuki Inui* and Masatoshi Suehiro*

(Received October 9, 1987)

Abstract

Carbon monoxide oxidation, steam reforming of methanol, C_3H_6 oxidation, and oxidation of the copper catalyst itself were performed by a flow method using copper catalysts with varying copper particle sizes ranging from 3.6 to 1700 nm in diameter. The specific rate of CO oxidation increased with a decreasing copper particle size. The specific rate of steam reforming of methanol increased with an increasing particle size in the small range within a 4-10 nm range, but this reaction was insensitive to increases in copper particle sizes greater than 10 nm. The selectivity for acrolein formation from C_3H_6 oxidation was maximum when the copper particle sizes were on the order of 20-80 nm in diameter, where the oxidation state of the copper during the reaction was near that of cuprous oxide. From these results, the following new concept was derived. The metal particle size in metallic catalysts controls the balance between the oxidation of copper and the reducing action of reactants or products during reactions involving oxygen.

1. Introduction

Since an early report on the hydrogenation of cyclopropane to propane over platinum catalysts[1], the effects of metal particle size on the catalytic activity have been extensively studied. Boudart has classified catalytic reactions on metallic catalysts into two categories[2]: One is termed "facile" or "structure insensitive" reactions in which the specific activity, the activity per unit metal surface area, or turnover frequency, molecules formed per surface metal atom per second, is independent of the metal particle size. The other is termed "demanding" or "structure sensitive" reactions in which specific activity is dependent upon the metal particle size. Efforts have been concentrated on studies of the

---

* Department of hydrocarbon Chemistry, Faculty of engeneering, Kyoto University, Sakyo-ku, Kyoto, 606, Japan

differences in catalytic reactions under reductive circumstances, such as hydrogenation [1),3)~6)], hydrogenolysis[7)~15)], isomerization[16)~18)], or deuterium exchange reactions[5),19)] over supported platinum or nickel catalysts. These reactions primarily involve the participation of hydrogen.

On the contrary, the effects of the metal particle size in metallic catalysts on catalytic oxidation and catalytic reactions with oxygen containing compounds have not been extensively studied. Studies that have been made in this area are summarized in Table 1. As can be seen from this summary, inconsistent results have been reported. For example, Wu et al.[20)] observed a negative dependence between the turnover frequency and silver particle size for the catalytic oxidation of ethylene. This means that the specific activity decreases with an increasing metal particle size. On the other hand, Jarjoui et al.[21)] reported a positive dependence for the same reaction. This apparent discrepancy may result from the following reason. During catalytic oxidation reactions, the oxidation state of the metal varies according to the reaction conditions, i.e. the temperature, the proportion of oxygen or oxygen containing reactants and the oxidation state of the catalyst metal at the beginning of the reaction[28)]. Conse-

Table 1   List of Works Studied on the Effect of Metal Particle Size on Oxidation Reactions

Reactant	Metal	Particle Size (A)	Reaction conditions			Result	Ref.
			Reactant (%)	O_2 (%)	Temp. (°C)		
C_2H_4	Ag	20−500	26.4	26.4	220	S(−)	(20)
C_2H_4	Ag	55−400	21.6	12.6	0−100	S(+)	(21)
CO	Pt	28, 78, 1000	0−2	98−100	208−280	S(+) in low CO	(22)
						I in high CO	
C_3H_6	Pt	11, 60, 144	0.1−2	20	220	S(+)	(23)
C_3H_6	Pt	20−2000	1	35	150−300	S(+)	(24)
H_2	Pt	(0.14−1.0)[a]	$H_2 \gg O_2$; $H_2/O_2 = 10$		0−100	S(−) in $H_2 \gg O_2$ I in $O_2 \gg H_2$	(25)
NH_3	Pt	20−155	$O_2 \gg H_2$: $O_2/H_2 = 6$		120−200	S(+)	(26)
EtOH	Pt					S(−)	(27)

S(+); The specific activity increases with increasing metal particle size (positive structure-sensitive).

S(−); The specific activity increases with decreasing metal particle size (negative structure-sensitive).

I ; The specific activity does not depend on metal particle size (structure-insensitive).

a ; dispersion.

quently, the adsorption state of reactants and/or products changes[28]. For example, Yao and Shelef reported that the oxidation state and the dispersion of rhodium, supported on γ–alumina, affects the adsorption of H_2, CO, and NO[29], indicating that the state of the metal surface, prior to and during the reaction, is very important, especially for oxidation reactions.

The relationship between the catalytic performance and oxidation state for various metal particle sizes was investigated in this study, using copper as a model catalyst. Because copper is oxidized or reduced more easily than platinum or nickel, the oxidation state of the copper surface during the reaction easily varies under the given reaction conditions for oxidation reactions[28]. The following three reactions were chosen as model reactions involving oxygen: (a) CO oxidation, (b) steam reforming of methanol, and (c) C_3H_6 oxidation.

2. Experimental

2.1. Catalysts

Catalysts were prepared by impregnation of γ–alumina, silica–alumina, or silica gel with an aqueous solution of research grade cupric nitrate. The BET–surface areas for these supports were 177, 1.6, and 465 m^2/g, respectively. The impregnated material was dried at ambient temperature for a few hours, followed by heating up to 500° C in air to decompose the cupric nitrate to CuO. The oxide was then reduced at 500° C in an electric furnace in a flow of 10% H_2 diluted with He for 30 min. Different copper particle sizes on the supported catalysts were obtained by varying the copper loading from 0.8 to 15 wt%. The copper powder, with a mean particle diameter 1700 nm, was a commercial lot produced by an electrolysis method.

2.2. Reaction Apparatus and Procedure

The reactions were carried out at atmospheric pressure in a continuous fixed bed flow reactor. The tubular Pyrex reactor was 5.0 mm in inner diameter and 40 cm in length, and heated by an electric furnace. The temperature was measured by a thermocouple located at the center of the catalyst bed. During the methanol steam–reforming, a gaseous mixture of methanol and steam was produced by evaporating a liquid mixture of methanol and water fed by a micro–tube pump. A 0.30 g portion of the pre–reduced catalyst was placed at the center of the reactor, and before each reaction re–reduced at 350° C for 10 min with 10% H_2 diluted with N_2. The reaction conditions, for the three kinds of reactions studied, are listed in Table 2. The products were analyzed by gas chromatogra-

Table 2   List of Reaction Conditions

Reaction	Temperature (°C)	Partial pressure (atm)	Space velocity (h^{-1})
CO oxidation (Fig. 3)	180	CO: 0.14 O$_2$: 0.0071	10^5
Methanol Steam–Reforming (Fig. 4)	180	CH$_3$OH: 0.05	3×10^3
C$_3$H$_6$ Oxidation (Fig. 5)	300	C$_3$H$_6$: 0.15 O$_2$: 0.05 H$_2$O: 0.02	5.8×10^4

phy with columns of MS–5 A, porapak T, or 30% polyethylene glycol 6000 supported on Celite 545.

2.3. Measurements of Metal Particle Size

In order to determine the specific free–metal surface area of reduced copper, CO adsorption measurements were performed by a chromatographic technique. A schematic diagram of the apparatus used is shown in Fig. 1. The catalyst, 0.3 ± 0.01 g, was placed in a Pyrex reactor surrounded by an electric heater. The temperature was measured by a thermocouple well inserted into the catalyst bed. The carrier gas (He) was purified by passage through an MS–5 A trap immersed
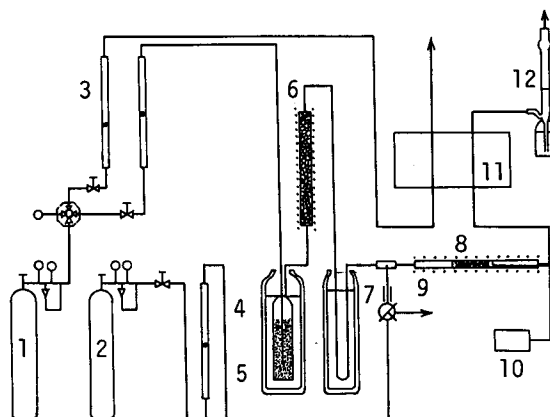

Fig. 1.   Schematic diagram of CO–adsorption apparatus.
1. He cylinder   2. H$_2$ cylinder   3. flow meter   4. liquid–N$_2$ bath   5. MS–5 A trap   6. deoxygenator packed with reduced Cu   7. dry–ice bath   8. sample cell   9. heater   10. pyrometer   11. gas chromatograph   12. soap–film flow meter.

in liquid nitrogen, and an oxygen absorber filled with SiO_2/Al_2O_3 supported Cu heated at 400° C. By this procedure, water and oxygen in the carrier gas were eliminated sufficiently to obtain reproducible results. The catalysts were first pretreated at 350° C for 10 min with extra pure H_2 (99.99999%) diluted with H_e. The excess H_2 was purged for 2 min at the same temperature, and the catalyst was cooled to room temperature. Pulses of CO of known volume were injected into the helium stream using a microsyringe. The eluted CO was measured by means of a thermal conductivity detector connected to an integrator. The amount of CO adsorbed onto the catalyst was calculated from the difference between the volume of the injected CO and that of the eluted CO. The mean particle size of copper ($\bar{d}$) was calculated as follows, assuming that all particles were spheres:

$$\bar{d} = \frac{6}{\rho \cdot S}, \qquad S = aNS'$$

where ρ=specific gravity of copper, S=metal surface area ($m^2/g-Cu$), a= amount of CO adsorbed (mol/g−cat), N=Avogadro number, and S'=cross− sectional area of a CO molecule ($13 A^2$).

2. 4. Oxidation Characteristics of Reduced Copper Catalysts

Measurements of oxidation rates were made using a Shimadzu micro–thermogravimetric analyzer TG–20 (tolerance 1 μg) with a gas–flow control and a gas–purification system. Details of the apparatus and the procedures have been described previously[28]. Oxidation was carried out at 180° C with a gas mixture of 8 % O_2− 92% N_2. A 30 mg portion of catalyst was used.

3. Results and Discussion

3. 1. Oxidation Rate Characteristics of Copper

Since the oxidation state of the catalyst metal during reactions is a very important factor determining the catalyst performance, the measurement of the initial oxidation rates of the reduced copper supported on silica or silica–alumina was considered to be important for the surface characteristic of the copper catalysts.

The oxidation rates of copper samples with different particle sizes are plotted in Fig. 2, using the Elovich equation coordinates. This type of representation of oxidation rates has been used to describe rate processes such as the oxidation of copper metal or the reduction of copper oxide[30],[31], and the adsorp-
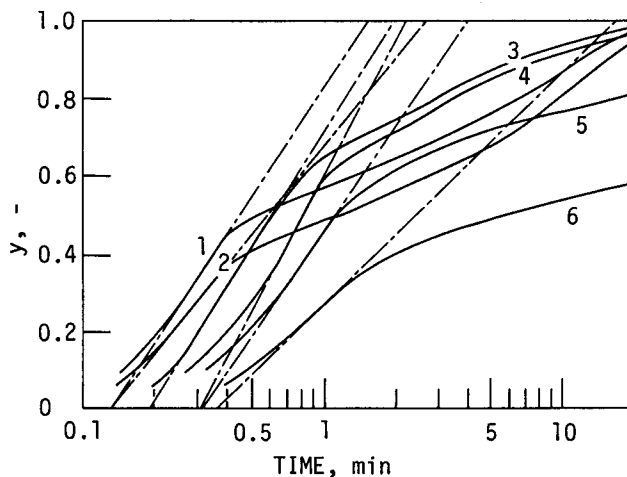
Fig. 2. Elovich plots for the oxidation of Cu with various particle sizes.
Copper particle size(nm) : 1, 3.6 ; 2, 4.9 ; 3, 6.8 ; 4, 10.6 ; 5, 14.2 ;
and 6, 19.9.

tion of nitrous oxide on copper or on nickel oxide[32),33)]. The Elovich equation in integral form is as follows:

$$y = \frac{2.3}{\alpha} \log t + \frac{2.3}{\alpha} \log (\alpha k)$$

where y is defined as the oxidized fraction (CuO_y), α is a coefficient of oxida-
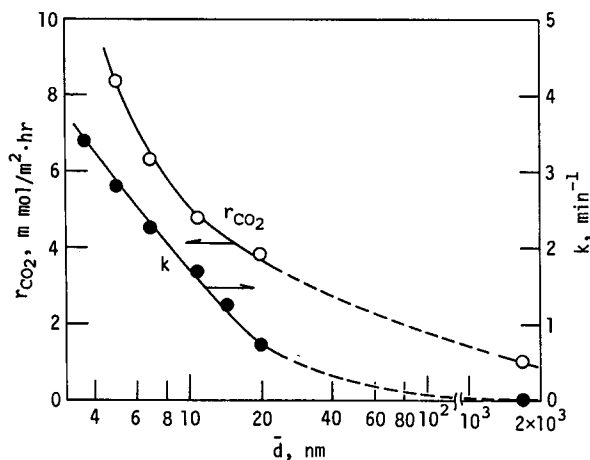

Fig. 3. Efect of copper particle size($\bar{d}$) on stoichiometric Cu oxidation(k) and catalytic CO oxidation(r_{CO_2}).
k ; initial oxidation rate of Cu.
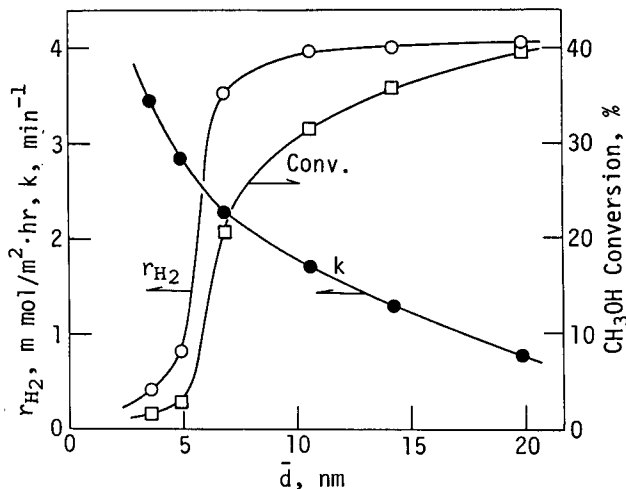r_{CO_2} ; specific rate of CO$_2$ formation in CO oxidation.

Fig. 4. Effect of copper particle size($\bar{d}$) on the specific rate of H_2 formation in steam-reforming of methanol(r_{H_2}) and initial rate of stoichiometric Cu oxidation(k).
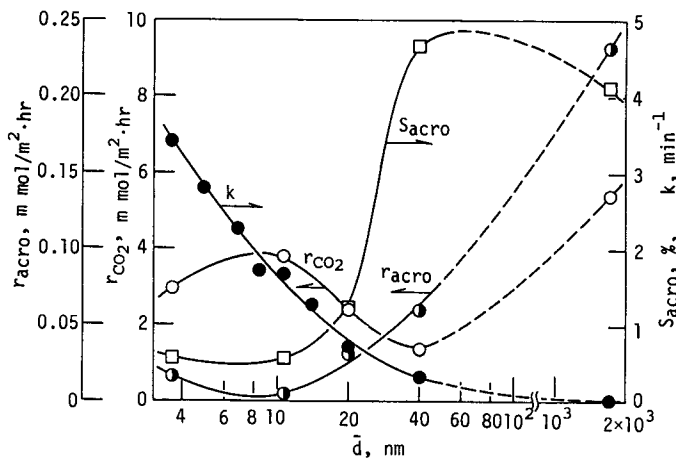

Fig. 5. Effect of copper particle size($\bar{d}$) on the C_3H_6 oxidation and initial rate of stoichiometric Cu oxidation(k).
r_{acro}; specific rate of acrolein formation in C_3H_6 oxidation.
r_{CO_2}; specific rate of CO_2 formation in C_3H_6 oxidation.
S_{acro}; selectivity to acrolein.

tion rate decrease, and k is the initial oxidation rate. The oxidized fraction, y, is obtained from the weight gain of the sample, α from the slope of the linear portions of y vs. log t in the early stages of oxidation, and k from the intercept of the extrapolated linear portions of y vs. log t at y = 0, i. e., the induction

period $= (\alpha k)^{-1}$.

The initial oxidation rate of copper, k, was calculated from the results in Fig. 2, and is shown in Figs. 3-5 as a function of the copper particle size ($\bar{d}$). The value of k decreases with an increasing $\bar{d}$, indicating that copper particles are more easily oxidized as their sizes are decreased. The relationships between the initial oxidation rates of the catalyst copper particles and specific activities were investigated for CO oxidation (Fig. 3), methanol steam–reforming (Fig. 4), and C_3H_6 oxidation (Fig. 5).

3.2. CO Oxidation

McCarthy et al.[22] found, at low CO partial pressure, the specific reaction rates of CO oxidation increased by increasing the platinum particle size as shown in Table 1.

Our results on CO oxidation over copper are shown in Fig. 3 where r_{CO_2} represents the steady–state specific reaction rate, expressed as moles of CO_2 formed per unit reduced copper surface area per unit of time. To avoid limiting the effects of mass transfer, the reactions were conducted under conditions in which the temperature dependence of r_{CO_2} was linear by Arrhenius plots. No catalyst deactivation was observed under the conditions.

The value of r_{CO_2} decreases with increasing values of $\bar{d}$, and there was a narrow correlation between r_{CO_2} and k (Fig. 3). The results suggest that in CO rich conditions (Table 2), the reductive action of CO is so strong[35] that the copper remains in a reduced state even when the copper particle sizes are small. This would result in a rapid rate of oxygen adsorption, and consequently, a more rapid rate of CO oxidation.

The results obtained here differ from those by McCarthy et al. They found that the catalytic oxidation of CO on a metallic catalyst to be structure sensitive. That is to say, the turnover frequency increases with increasing platinum particle sizes. As pointed out by Hanson and Boudart[25], the difference in gas composition seem to have affected the catalytic behavior. Hanson and Boudart investigated the oxidation of hydrogen over silica supported platinum under conditions of excess oxygen or excess hydrogen. They found the reaction to be structure–insensitive in excess oxygen but structure–sensitive in excess hydrogen. Consequently, they considered the possibility of corrosive chemisorption[34] by oxygen in excess. In excess oxygen, surface anisotropies are eliminated due to the high binding energy of chemisorbed oxygen, because of the smaller binding energy of hydrogen. The results obtained in this study with excess CO are similar to those of Hanson and Boudart when they used excess hydrogen

conditions, i. e., the specific activity or turnover frequency of the metal catalyst increases with decreasing metal particle size. This fact supports the finding of Hanson and Boudart, and extends their observations to catalytic oxidation reactions.

3. 3. Steam Reforming of Methanol

Kobayashi et al.[36] reported recently that the turnover frequency for steam reforming of methanol using supported Cu catalysts did not depend on the copper particle size in the range of 15 to 319 nm in diameter.

In the present study, the influence of the copper particle size on the specific rate of hydrogen formation, r_{H2}, according to the equation $CH_3OH + H_2O \rightarrow 3 H_2 + CO_2$ is shown in Fig. 4. The value of r_{H_2} was extremely small in the $\bar{d}$ range of < 4 nm, then increased abruptly with an increasing $\bar{d}$, and finally reached the maximum value when the value of $\bar{d}$ was more than 8 nm. It is noted that this reaction on alumina supported Cu catalysts is structure sensitive for copper particles with diameters within 4 and 10 nm, and insensitive in the range of more than 10 nm. Our results are consistent with the results of Kobayashi et al. mentioned above for copper particle sizes larger than 10 nm in diameter.

3. 4. C₃H₆ Oxidation

It is well known that the selective oxidation of propylene to acrolein is most active when the catalyst copper is in the form of cuprous oxide[38]~[40]. For example, it has been reported that the highest acrolein selectivity is obtained by adding a small concentration of selenium vapor to the reaction gases[41],[42]. The role of selenium has been elucidated as a reducing agent for cupric oxide to cuprous oxide[43]. These results indicate that the oxidation state of copper influences the catalytic activity and acrolein selectivity for propylene oxidation. The particle size of copper is anticipated to affect the oxidation state of copper according to the specific reaction conditions. Carballo and Wolf[23] studied the effects of particle size during the complete oxidation of C_3H_6 on γ-alumina supported platinum catalysts under conditions of a low C_3H_6 concentration and a large excess of oxygen. They showed that the reaction was extremely sensitive to platinum particle sizes[23].

In this study, propylene oxidation on copper catalysts was carried out under conditions of excess propylene. The results are shown in Fig. 5. Oxidation products were mainly acrolein and carbon dioxide with very small amounts of acetaldehyde and acetone. It can be seen in this figure that the rate of formation of acrolein, r_{acro}, increased with an increasing d. On the other hand, r_{CO_2} first

Table 3 Oxidation State of Cu with Various Particle Sizes and Its Parformance in C_3H_6 Oxidation

Catalyst	$\bar{d}$ (nm)	$y^{1)}$ (−)	r_{acro} (mmol/m^2 · h)	r_{CO_2} (mmol/m^2 · h)	$S_{acro}^{2)}$ (%)
15%Cu/SiO$_2$	8	0.69	0.65	2.14	16.1
10%Cu/SiO$_2$−Al$_2$O$_3$	40	0.41	0.51	0.49	50.0
Cu powder	1,700	0.20	1.23	4.87	20.0

1) y is defined as the fraction oxidized (CuO$_y$) at the steady-state reaction.
2) Selectivity based on converted propylene.

decreased with an increasing $\bar{d}$ when $\bar{d}$ was between 10 and 40 nm and increased with an increasing $\bar{d}$ when $\bar{d}$ was greater than 40 nm. When $\bar{d}$ was less than 10 nm, r_{CO_2} decreased probably due to the formation of a CuO layer. For this reason, selectivity to acrolein, s_{acro}, presents a maximum for $\bar{d}$ around 40 nm (Fig. 5).

In order to investigate the oxidation state of copper during the C_3H_6 reaction, a micro-thermogravimetric analyzer was used. The reaction values of the steady state after 70 min on stream are shown in Table 3. The results are similar to those in Fig. 5 ; y increased with a decreasing $\bar{d}$. The ratio of combustion rate was relatively large for $\bar{d}$ of both 8 and 1700 nm. Accordingly, the optimum particle size and oxidation state of the catalyst copper for maximum S_{acro} were around 40 nm and CuO$_{0.4}$, respectively. Therefore, the effect of copper particle size on propylene oxidation is not so simple as the results of Carballo and Wolf would suggest[28], due to the retardation caused by adsorption of reactants and products. However, it is well understood from the dependence of k with $\bar{d}$ that when the copper particle size is small, the oxidation rate of copper is higher. The oxidation state of copper would be high (CuO) and propylene oxidation would go to completion to form mainly carbon dioxide. With an increasing copper particle size the oxidation rate of copper decreases, and the resulting oxidation state of copper would be closer to Cu_2O promoting an increased formation rate for acrolein.

4. Conclusion

The effects of metal particle size on catalytic activity for oxidation reactions and reactions with oxygen containing compounds are dependent upon the oxidation state of the catalyst metal during catalytic reactions. According to this new concept, it is understood that when the catalyst metal is in a reduced state,

hydrogenation and isomerization of hydrocarbon proceed more effectively. However, when the catalyst surface is in the oxidized state the effect often gives a contrary result to that of hydrogenation etc. The oxidation state is produced by various factors such as metal particle size, composition of the gas feed, temperature, and retardative action of reactants and/or products. Thus, the apparent discrepancies for the different catalysts and reactions that have been reported previously may be consistently explained on the basis of the new concept presented in this paper.

References

1) M. Boudart, A. Aldag, J. E. Benson, N. A. Dougharty, and G. C. Harkins, J. Catal. **6**, 92 (1966).
2) M. Boudart, Adv. Catal. **20**, 153 (1969).
3) P. Ratnasamy, J. Catal. **31**, 466 (1973).
4) T. A. Dorling, and R. L. Moss, J. Catal. **5**, 111 (1966).
5) R. Mauel, G. Leclercq, and J. Barbier, J. Catal. **37**, 324 (1975).
6) S. Fuentes, and F. Figueras, J. Catal. **61**, 443 (1980).
7) D. J. C. Yates, W. F. Taylor, and J. H. Sinfelt, J. Amer. Chem. Soc. **86**, 2996 (1964).
8) W. F. Taylor, J. H. Sinfelt, and D. J. C. Yates, J. Phys. Chem. **69**, 3857 (1965).
9) D. J. C. Yates, and J. H. Shinfelt, J. Catal. **8**, 348 (1967).
10) Y. L. Lam, and J. H. Sinfelt, J. Catal. **42**, 319 (1976).
11) Yu. A. Ryndin, B. N. Kuznetsov, and Yu. I. Yermakov, Kinet. Catal. Lett. **7**, 105 (1977).
12) A. Sarkany, and P. Tetenyi, React. Kinet. Catal. Lett. **12**, 297 (1979).
13) H. C. Yao, Y. F. Yao, and K. Otto, J. Catal. **56**, 21 (1979).
14) G. A. Martin, J. Catal. **60**, 452 (1979).
15) M. F. Guilleux, J. A. Dalmon, and G. A. Martin, J. Catal. **62**, 235 (1980).
16) M. Boudart, A. W. Aldag, L. D. Ptak, and J. E. Benson, J. Catal. **11**, 35 (1968).
17) F. M. Dautzenberg and J. C. Platteeuw, J. Catal. **19**, 41 (1970).
18) J. M. Dartigues, A. Chambellan, and F. G. Gault, J. Amer. Chem. Soc. **98**, 856 (1976).
19) O. M. Poltorak and V. S. Boronin, Russ. J. Phys. Chem. (English Transl.) **39**, 1329 (1965).
20) J. C. Wu and P. Harriott, J. Catal. **39**, 395 (1975).
21) M. Jarjoui, P. C. Gravelle, and S. J. Teichner, J. Chem. Phys. **75**, 1069 (1978).
22) E. McCarthy, J. Zahradnik, G. C. Kuczynski, and J. J. Carberry, J. Catal. **39**, 29 (1975).
23) L. M. Carballo and E. E. Wolf, J. Catal. **53**, 366 (1978).
24) Y. Tokoro, K. Hori, T. Nagira, T. Uchijima, and Y. Yoneda, Nippon Kagaku Kaishi 1646 (1979).
25) F. V. Hanson, and M. Boudart, J. Catal. **53**, 56 (1978).
26) J. J. Ostermaier, J. R. Katzer, and W. H. Manoque, J. Catal. **33**, 457 (1974).
27) O. M. Poltorak, U. S. Bornin, and A. M. Mitrofarova, Proc. Int. Congr. Catal. 4 th, (Moscow) 1968, **2**, 276 (1971).
28) T. Inui, T. Ueda, and M. Suehiro, J. Catal. **65**, 166 (1980).
29) H. C. Yao, S. Japar, and M. Shelef, J. Catal. **50**, 407 (1977).

30) H. H. Voge and L. H. Atkins, J. Catal. **1**, 171 (1962).

31) T. Inui, T. Ueda, M. Suehiro, and H. Shingu, J. Chem. Soc., Faraday Trans. 1. **74**, 2490 (1978).

32) H. S. Gandhi and M. Shelef, J. Catal. **24**, 241 (1972).

33) H. S. Gandhi and M. Shelef, J. Catal. **28**, 1 (1973).

34) J. Benard, Catal. Rev. **3**, 93 (1970).

35) T. Inui, T. Ueda, and M. Suehiro, Nippon Kagaku Kaishi, 934 (1977).

36) H. Kobayashi, N. Takezawa, and C. Minochi, J. Catal. **69**, 487 (1981).

37) T. Inui, M. Suehiro, and Y. Takegami, J. Japan Petrol. Inst. **25**, 63 (1982).

38) R. J. Sampson and D. Shooter, Oxid. Combust. Rev. **1**, 250 (1965).

39) H. H. Voge and C. R. Adams, Adv. Catal. **17**, 174 (1967).

40) B. J. Wood, H. Wise, and R. S. Yolloes, J. Catal. **15**, 355 (1969).

41) E. P. Goodings and D. J. Hadley, U. S. Pat. **2**, 593, 437 (1953).

42) N. Kominami, Kogyo Kagaku Zassi **65**, 1514 (1962).

43) N. Kominami, Kogyo Kagaku Zassi **65**, 1517 (1962).